

# Laser Studies for the Laser-Wire Scanner at PETRA-III

Thomas Aumeyr,\* Grahame A. Blair, Stewart T. Boogert, Gary Boorman, and Alessio Bosco  
*Royal Holloway, University of London*

Klaus Balewski, Vahagn Gharibyan, Gero Kube, and Kay Wittenburg  
*DESY, Hamburg*  
 (Dated: December 14, 2011)

The PETRA-III Laser-wire, a Compton scattering beam size measurement system at DESY, uses an automated mirror to scan a Q-switched laser across the electron beam and is developed from the system previously operated at PETRA-II. This paper reports on recent results on intensive laser studies and presents improvements on the laser pulse fittings.

## I. INTRODUCTION

Laser-wire (LW) beam profile monitors will be the key beam diagnostic instruments for future very high energy/intensity particle accelerators to replace the use of traditional profiling techniques such as wire scanners or screens. LWs can be employed in synchrotron light sources [1], linear electron-positron colliders [2], and most recently  $H^-$  ion accelerators [3].

The principle of operation of a LW profiler is to map the spatial distribution of the particle bunch by using the signal produced in the collision between the particles and the photons of a laser beam scanned across the accelerated beam. In electron machines, using the Compton effect, the laser photons are scattered by the electrons and can be detected downstream as gamma rays in a calorimeter. At  $H^-$  machines, where the fundamental process is photo-ionization of the  $H^-$  ion to form neutral H-atoms, the released electrons can be detected downstream.

The LW system described in this paper was built at the PETRA-III accelerator at DESY in Hamburg (see Fig. 1). The LW system is an upgrade of the two-dimensional LW tested previously at the PETRA-II accelerator [1]. The updated LW includes features to make measurements more reliable, such as real time correction for laser pulse-to-pulse power fluctuation and time or position jitter. Furthermore, knife-edge scans to measure the laser spot size as it is at the interaction point (IP) can be performed on-demand, allowing the user to extract the contribution of the laser width from the total signal distribution.

The relevant beam parameters of PETRA-III are gathered in Table I. Also the expected horizontal and vertical beam sizes at the LW IP are stated.

TABLE I. PETRA-III machine parameters [4]

Parameter	Symbol	Value	Unit
Positron energy	$E$	6.0	GeV
Circumference	$C$	2304	m
Revolution frequency	$f_{rev}$	130.1	kHz
No. of bunches / fill	$N_{fill}$	960 and 40	
Bunch separation	$\Delta t_b$	8 and 192	ns
Positron beam current	$I_B$	100	mA
No. of positrons / bunch	$N_{e^+}$	0.5 and 12	$10^{10}$
Horizontal emittance	$\epsilon_x$	1	nm-rad (rms)
Coupling factor	$\kappa$	1	%
Vertical emittance	$\epsilon_y$	0.01	nm-rad (rms)
Energy spread	$\frac{\Delta E}{E}$	0.1	% (rms)
Exp. hor. beam size	$\sigma_x$	$\sim 175$	$\mu\text{m}$
Exp. vert. beam size	$\sigma_y$	$\sim 15$	$\mu\text{m}$

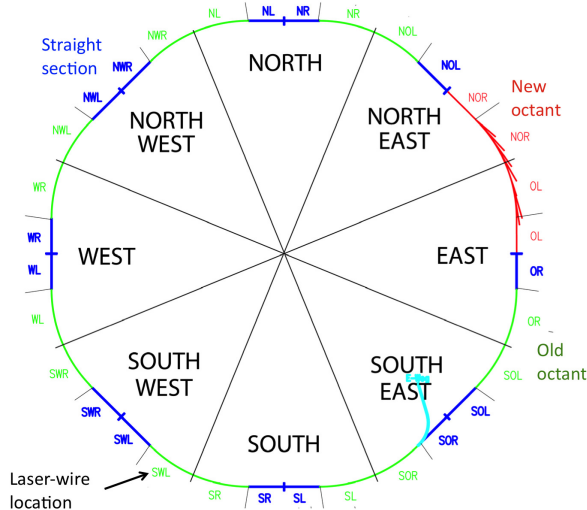


FIG. 1. LW location at the PETRA-III facility.

## II. SETUP

In Fig. 2, a plan overview of the LW experimental layout on the south-west bending arc of the PETRA-III ring is shown. It illustrates the major components of the LW system: high power laser, optical scanning systems, beam position monitor (BPM) and Compton calorimeter.

\* tom.aumeyr.2008@live.rhul.ac.uk

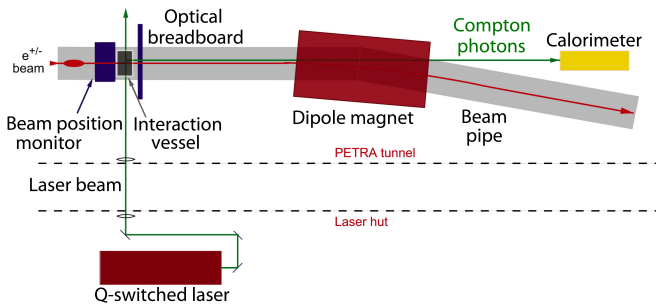


FIG. 2. Overview of the LW setup [1].

The laser pulse collides with the positron bunch within a custom built vacuum vessel with optical view ports for laser light. The Compton photons produced in the collisions between the positron bunches and the laser light are separated downstream from the particle beam by a dipole magnet. After separation, the Compton photons exit the beam pipe through an aluminium window to reduce the synchrotron radiation background and are detected by a calorimeter. The photon detector is made of nine lead tungstate crystals organised in a  $3 \times 3$  matrix which is optically connected to a photo-multiplier [1]. The position of the positron beam on either side of the IP is measured by a four-button pick-up BPM.

A Q-switched Nd:YAG laser system with a repetition rate of 20 Hz is used to produce the high power light pulses required for Compton scattering. The laser beam is expanded and collimated to approximately 25 mm diameter and transported from the laser hut into the accelerator tunnel underneath. The laser beam is then guided onto the LW breadboard mounted around the beam pipe, which contained the vertical (V) and horizontal (H) scanning systems. The LW scanning unit consists of a piezo-electric driven mirror that deflects the laser beam before it is focused by the scanning lens.

Fig. 3 and Fig. 4 show a schematic of the optical layout and a photo of the LW breadboard respectively. The arrows indicate movable transition stages. For the LW scanning system, two scanning lenses were chosen with different focal length. This was a necessary upgrade in order to match the different beam sizes and scan range requirements in the two profiling directions (V and H). The focussing lenses are an aplanatic lens with  $f = 250$  mm (LV) and a spherical singlet lens with  $f = 750$  mm (LH).

The scanning axis (V or H) is set by the position of the first movable mirror. The scanning mirrors (SV and SH) are identical for both axes. These are 2-inch mirrors mounted on a piezo-electric stack that can be deflected by applying a voltage. The maximum deflection angle is 2.5 mrad with an applied voltage of 100 V. Given the focal lengths of 250 mm and 750 mm, the total maximum scanning range is 1.25mm for the V axis and 3.75 mm for the H axis.

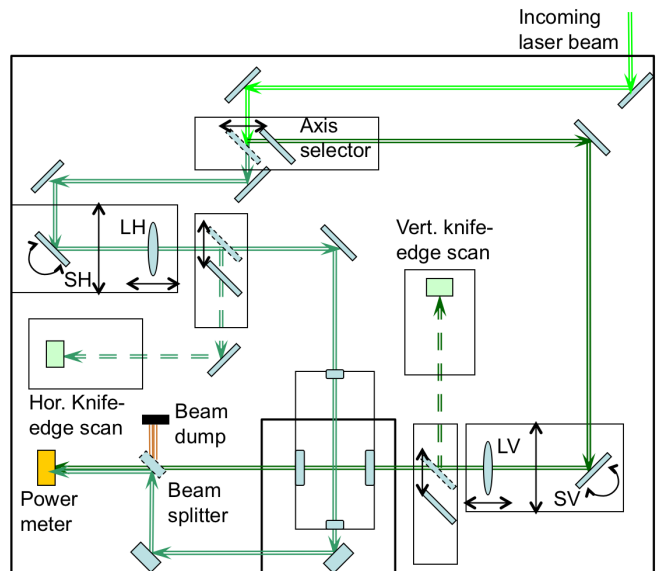


FIG. 3. Schematic layout of the vertical breadboard.

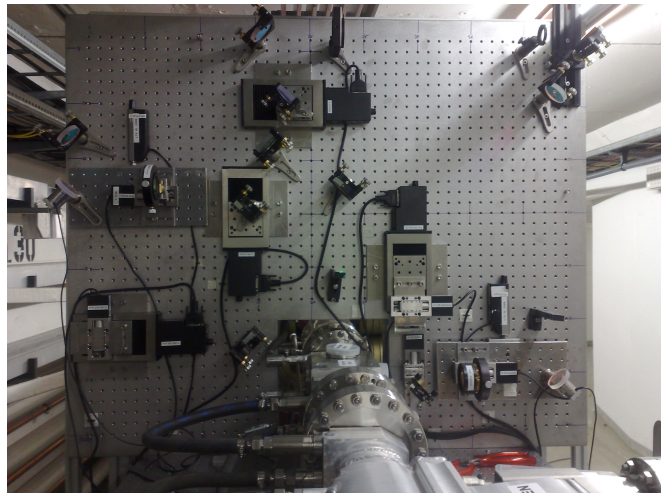


FIG. 4. Photo of the LW optical breadboard.

### III. LASER STUDIES

#### A. Transverse mode

The laser beam propagates longitudinally as described by

$$W(z) = W_0 \sqrt{1 + \left( \frac{(z - z_0)M^2\lambda}{\pi W_0^2} \right)^2}. \quad (1)$$

where  $W(z)$  is the laser waist defined as the distance from the centroid of the spot to the position where the intensity drops by a factor  $(\frac{1}{e^2})$ ,  $W_0$  is the minimum laser waist,  $\lambda$  is the laser wavelength and  $M^2$  is a factor  $\geq 1$  which represents the quality of the real beam

compared to an ideal TEM<sub>00</sub> Gaussian beam (for which  $M^2 = 1$ ) [1].

The longitudinal profile of the laser beam was measured by focusing it with the same lenses used for the actual setup at a location close to actual interaction point thus reproducing real conditions. CCD images of the laser beam were recorded using a laser diagnostic camera (Gentec WinCamD) at a range of distances from the focusing lens. An image of the laser intensity profile can be seen in Fig. 5. This shows the laser spot focussed by the LAP250 lens used for scanning in the vertical direction.

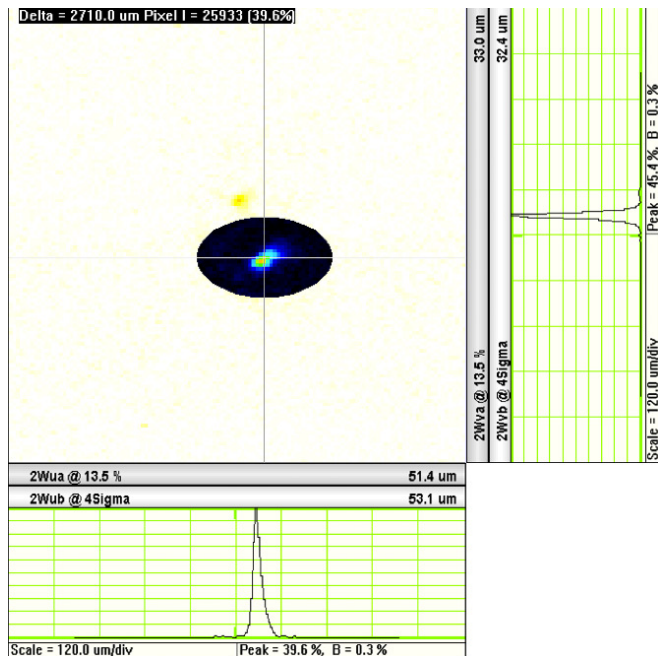


FIG. 5. Laser pulse image taken using CCD profiling equipment in the post IP section of the LW system.

The profiling software provides a 2D profile of the laser intensity, however only the horizontal projection is of importance as this is the direction in which the laser traverses while scanning. It can be seen that the laser pulse does not have a purely Gaussian profile, but shows a slight skew. For this reason, several CCD images were taken at each position, their horizontal profiles extracted and then fitted with a mode-mixing Gaussian function,

$$f(x) = A \exp\left(-\frac{(x - \mu)^2}{2\sigma^2}\right) (1 + b(x - \mu - \Delta)^2) + d. \quad (2)$$

This function takes a mixing of the first two laser modes into account which is described by a linear combination of the first two Hermite polynomials. As the laser modes are orthogonal, they are assumed to be incoherent and shifted by some offset  $\Delta$ . An example laser profile fitted with Eq. 2 is shown in Fig. 6.

The beam width data as a function of camera position are plotted in Fig. 7 and fit using Eq. 1. The  $M^2$  obtained from the fit was  $2.18 \pm 0.05$

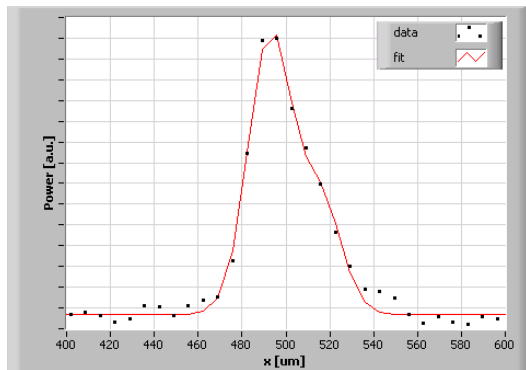


FIG. 6. Extracted horizontal laser pulse profile fitted with a mode-mixing-gaussian fit-function.

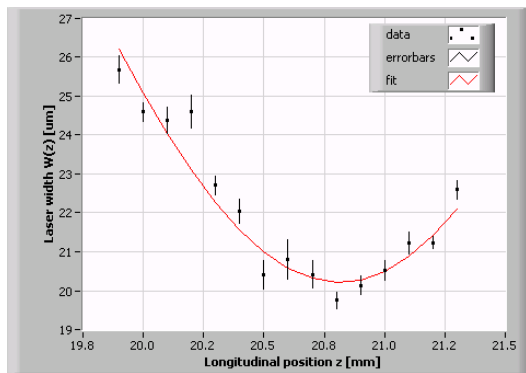


FIG. 7. Measurement of  $M^2$  using an LAP250 lens. The fit equation is given in Eq. 1. The fit gives  $M^2 = 2.18 \pm 0.05$ .

## B. Pointing jitter

Random, thermal vibrations occurring in the laser head cause the direction in which the laser pulse is fired from the laser to fluctuate [5]. This directional fluctuation is called pointing jitter.

The pointing jitter at the laser IP for both scanning directions was measured by deflecting the laser beam after the respective scanning lens and just before the entrance window of the vacuum chamber and putting a laser diagnostic camera (Gentec WinCamD) exactly in its focus point. The centroid positions of several consecutive laser shots were recorded and their values relative to their mean fill the histograms shown in Fig. 8 and Fig. 9.

Therefore the pointing jitter angle can be calculated using the RMS values from the histograms as  $1.97 \mu\text{m}/0.25 \text{ m} = 7.86 \mu\text{rad}$  for the vertical scan and  $6.56 \mu\text{m}/0.75 \text{ m} = 8.74 \mu\text{rad}$  for the horizontal scan.

## IV. CONCLUSIONS AND OUTLOOK

The PETRA-III LW system has already successfully performed horizontal and vertical beam size measurements [6]. Previous laser studies have been repeated in

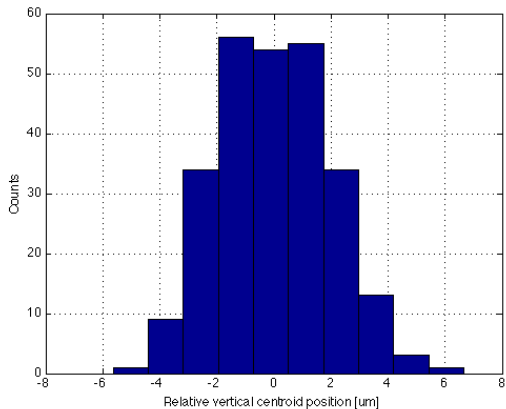


FIG. 8. Histogram showing the pointing jitter at the laser IP for the LAP250 lens.

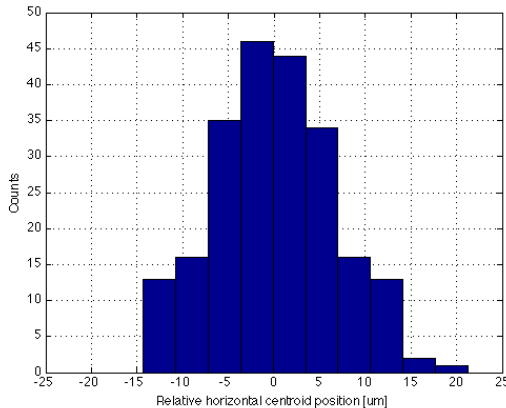


FIG. 9. Histogram showing the pointing jitter at the laser IP for the LAP750 lens.

more detail and understanding of the laser functionality has been improved.

The next steps are detailed revision of already acquired data and carrying out further benchmarking beam studies, e.g. to measure the lattice characteristics (dispersion, compaction factor, beta functions, etc.), compared with other beam size diagnostic instruments [7].

- 
- [1] A. Bosco *et al.*, Nucl. Instrum. Meth. A **592**, 162 (2008).  
 [2] I. Agapov, G. A. Blair, and M. Woodley, Phys. Rev. ST Accel. Beams **10**, 112801 (2007).  
 [3] Y. Liu *et al.*, EPAC'08 **TUPC061** (2008).

- [4] "Machine Parameters PETRA III (Design Values)," (2011).  
 [5] A. E. Siegman, *Lasers* (University Science Books, 1986).  
 [6] T. Aumeyr *et al.*, IPAC'10 **MOPE069** (2010).  
 [7] G. Kube *et al.*, IPAC'10 **MOPD089** (2010).